TALLINNA TEHNIKAÜLIKOOL
TALLINN UNIVERSITY OF TECHNOLOGY

Department of Materials and Environmental Technology

POST DEPOSITION THERMAL TREATMENT OF SPUTTERED ANTIMONY SELENIDE THIN FILMS

MAGNETRONPIHUSTATUD Sb_2Se_3 ÕHUKESTE KILEDE SADESTUSJÄRGSE TERMOTÖÖTLEMINE

MASTER THESIS

Student: Joseph Olanrewaju Adegite

Student code: 173971KAYM

Supervisor: Dr. Olga Volobujeva, Senior Research Scientist.
Dr. Svetlana Polivtseva, Researcher.

Tallinn, 2019

AUTHOR'S DECLARATION

Hereby I declare, that I have written this thesis independently.
No academic degree has been applied for based on this material. All works, major viewpoints and data of the other authors used in this thesis have been referenced.

"....." ..... 201.....

Author: Joseph Olanrewaju Adegite .....
/signature /

Thesis is in accordance with terms and requirements

"....." ..... 201....

Supervisor: Olga Volobujeva .....
/signature/

Co - Supervisor: Svetlana Polivtseva .....
/signature/

Accepted for defence

"....."..... 201... .
Chairman of theses defence commission: .....
/name and signature/

Department of Materials and Environmental Technology

THESIS TASK

Student: Joseph Olanrewaju Adegite, 173971KAYM

Study programme: Materials and Processes of Sustainable Energetics

Main speciality: Processes of Sustainable Energetics

Supervisors: Senior Research Scientist, Dr. Olga Volobujeva, +3726203368

Researcher, Dr. Svetlana Polivtseva, +3726203368

Thesis topic:

Post deposition thermal treatment of sputtered antimony selenide thin films

Magnetronpihustatud Sb_2Se_3 õhukeste kilede sadestusjärgse termotöötlemine

Thesis main objectives:

1. To investigate the influence of deposition temperatures on properties of Sb_2Se_3 thin films deposited by RF Magnetron Sputtering deposition technique.
2. To study the influence of post-deposition thermal treatment in Ar-Se atmosphere on the properties of sputtered Sb_2Se_3 thin films.

Thesis tasks and time schedule:

No	Task description	Deadline
1.	Deposition of Sb_2Se_3 silms on SLG and SLG-Mo Substrate by Magentron sputtering at different substrate temperatures	
2.	As deposited Sb_2Se_3 film characterization by SEM/EDS, Raman, UV-Vis Spectroscopy and XRD	
3.	Annealing of Sb_2Se_3 film deposted at 300^{o}C in Ar-Se atmosphere, at different annealing temperatures	
4.	Annealed Sb_2Se_3 film characterization by SEM/EDS, Raman, UV-Vis Spectroscopy, XRD, Kelvin probe, electrical measurement	
5.	Solar cell fabrication and performance evaluation.	

Language: English **Deadline for submission of thesis:** " 27th " May 2019.

Student: Joseph Olanrewaju Adegite ..... "....."....201....

/signature/

Supervisor: Olga Volobujeva ..... "....."....201....

/signature/

Co-supervisor: Svetlana Polivtseva ..... "....."....201....

/signature/

Terms of thesis closed defence and/or restricted access conditions to be formulated on the reverse side

TABLE OF CONTENTS

PREFACE

In this work, we first investigated the influence of deposition temperatures on the properties of Sb_2Se_3 thin films produced using magnetron sputtering deposition technique and in the second part of this work we studied the influence of post deposition thermal treatment of the sputtered Sb_2Se_3 films in Ar-Se atmosphere. Thin films of Sb_2Se_3 were deposited on different substrates at different substrate temperatures. The produced films were then characterized using different techniques. Result showed that film deposited at RT was amorphous, while there exists some crystallinity in the film deposited at higher temperatures, film quality also improved as the temperature increased. Bang gap of obtained films decreased from 1.75eV to 1.25eV as the deposition temperature increased. For the second part of the experiment, the best Sb_2Se_3 film fabricated from the first part was annealed in Ar-Se atmosphere in isothermal sealed quartz ampoules at different annealing temperatures. Result showed a further decrease in band gap value, improved photosensitivity, improvement in selenium deficiency and overall film quality as annealing temperatures increased. Sb_2Se_3 film with the best quality after both investigations was then made into a solar cell with structure graphite/ZnO:AL/i-ZnO/CdS/Sb_2Se_3/Mo and after testing the following solar cell parameters; $I_{SC;}$ 11.6mA/cm^2, V_{OC}; 233.85mV, fill factor, 28.2% and solar cell efficiency of 0.763%. were recorded.

I would like to thank my supervisor, Dr. Olga Volobujeva for her professional expertise and advice as well as motherly and friendly care towards me all through this period, special thanks also goes to my Co supervisor Dr. Svetlana Polivtseva, without them both I would not have completed this work, they guided through structuring the experiment and also the report writing. I also like to thank Dr. Sergie Bereznev for all his advisory role, Jaan Raudoja for help with annealing's, Dr. Marit Kauk-Kuusik and Dr. Maris Pilvet for helping with the solar cell fabrication and parameters measurement and finally Dr. Nicolae Spalatu for his help with XRD analysis.

This work is financially supported by the Estonian Research Council Foundation under the title PUT1485 SnS and SnSe thin films for solar energy. My sincere gratitude goes to the Estonian government and Tallinn University of Technology for supporting my studies and research through the tuition waiver, Dora, Speciality, Needs based and Performance scholarships.

Keywords: Sb_2Se_3, Magnetron sputtering, Argon-Selenium, As-deposited, Annealing.

LIST OF ABBREVIATIONS AND SYMBOLS

Sb_2Se_3	Antimony Selenide
Ar	Argon
Se	Selenium
SEM	Scanning electron microscopy
EDS/EDX	Energy dispersive X-ray spectroscopy
XRD	X-ray Diffraction
I_{SC}	Short circuit current
V_{OC}	Open circuit voltage
Mo	Molybdenum
SLG	Soda lime glass
PV	Photovoltaics
PVD	Physical vapour deposition
UV-Vis	Ultraviolet-Visible
E_g	Optical energy band gap
RT	Room temperature

Table of Figures.

Introduction

The world has always and will always need energy for its survival, over the years we have strongly depended on fossils for our energy needs, however, recent reports have shown that fossil resources will soon be exhausted, it has also been proven to not be a sustainable source of energy; it is limited by its environmental impact on the world at large and several countries have gathered and agreed to reduce and even stop their dependence on fossil. Several sustainable alternatives to fossil have been provided [1]. Of these alternatives solar energy stands out for its abundance, energy absorbed from the sun by the earth in an hour can supply the earth energy need for a year, solar energy for electricity generation (PV) requires the use of solar cells, hence, produce no noise during use, requires little maintenance, can be used remotely and for small applications and they produce no greenhouse gases during use [1, 2].

Solar cells or photovoltaic cells currently exist in three generations: The first generation which is made up of mono and poly crystalline silicon cells, they have high efficiencies, but the production is expensive and complex, possesses low absorption coefficient and are heavier and more expensive. The second-generation solar cells are referred to as the thin film solar cells and they include the amorphous silicon, cadmium telluride, copper indium gallium di-selenide and others. They are more economical and easier to manufacture, they weigh less, use less materials and cost less per watt, they also have higher absorption coefficient when compared with the 1st generation cells. The third-generation cells include Nano crystal based, polymer based, dye sensitized and concentrated solar cells, they are not yet commercially available [1 – 4].

The current most efficient second-generation solar cells although performance wise are close to those of the first generation, they are however limited by the type of materials they use, the continuous availability of Gallium, Indium and Tellurium is unlikely and some of these materials are toxic to nature [5]. Therefore, there is a need to replace these materials with more abundant, less toxic and at least equally efficient materials. Antimony selenide (Sb_2Se_3) fits well into this category, it has a huge potential to be the absorber layer of future solar cells, it has quite simple composition, suitable electronic properties, appropriate bandgap as well as its abundance nature and no toxicity risk.

Present work is focused on investigating the influence of deposition temperatures on properties of Sb_2Se_3 thin films in RF Magnetron Sputtering and also to study the influence of post-deposition thermal treatment in Ar-Se atmosphere on the properties of sputtered Sb_2Se_3 thin films. There are few studies on the fabrication of Sb_2Se_3 films using the magnetron sputtering deposition technique, which has a great

potential to produce uniform and well-adhered films with controlled impurities content. In the literature, there is still a lack of knowledge on post-deposition treatment suitable for Sb_2Se_3 thin films. The following work is organized as follows:

- Chapter one: provides information about Sb_2Se_3, explains the different growth techniques that have been utilized so far in the development of Sb_2Se_3 thin films, provides up to date review of literature of various investigation done on Sb_2Se_3 solar cells.
- Chapter two: explains the experimental procedures followed in the current investigation.
- Chapter three: presents the result of this investigation and attempts to discuss them.
- Chapter four: provides the conclusion for this investigation.

CHAPTER ONE: LITERATURE REVIEW

1.1. Antimony selenide (Sb_2Se_3).

Phase Diagram.

Antimony (Sb) as an element in group 15 of the periodic table exhibits multiple oxidation state varying from -3 to +5. The highest oxidation state of +5 is slightly more stable than +3. Thus, a variety of Sb (III) and Sb(V) compounds are known to exist [6 - 8]. The equilibrium Sb-Se phase diagram depicts just one thermodynamically stable antimony selenide, Sb_2Se_3 phase comprising ~40 at. % of Sb (Figure 1) [9].

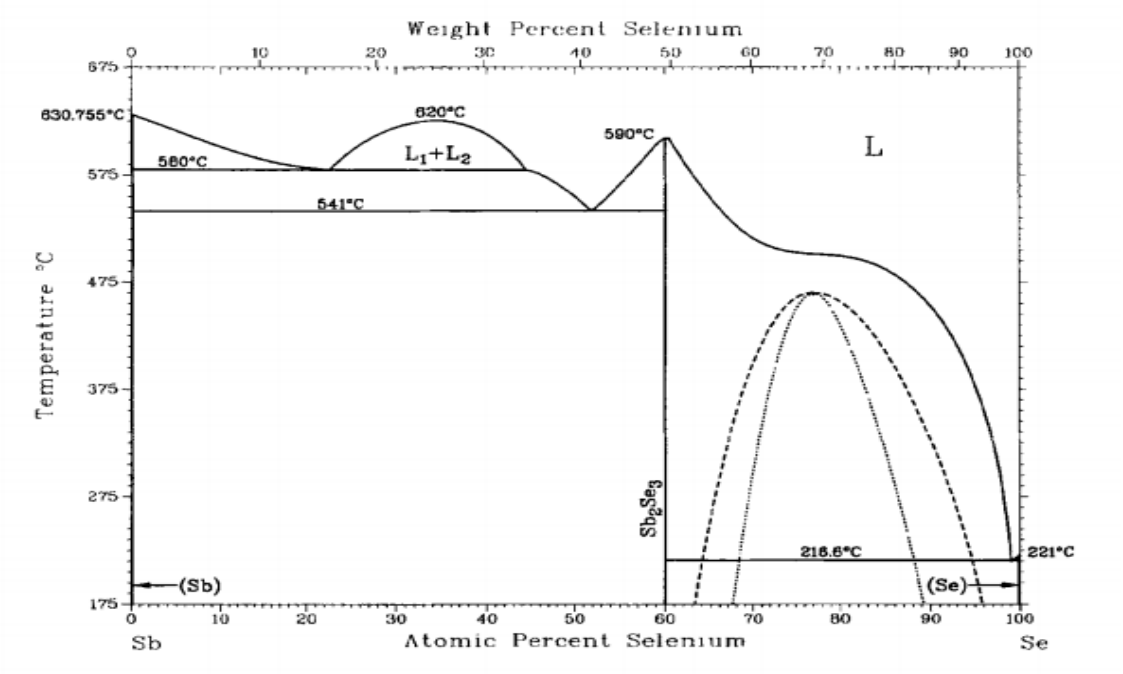

Figure 1 - Antimony - Selenium Phase Diagram [9]

Crystal Structure.

Sb_2Se_3 crystallizes in the orthorhombic Pnma structure at temperatures below 590 ^oC (Figure 1). Orthorhombic Sb_2Se_3 is isostructural to antimony sulfide (Sb2S3) and bismuth sulfide (Bi_2S_3), having a=12.84 Å, b=11.77 Å and c=4.03Å [10]. Each unit cell contains four molecules and shows very low-symmetric environment (both Sb and Se atoms). The unit cell has a one-dimensional chain structure in

the b- axis with atomic contacts linking each one-dimensional chain to give the 3D orthorhombic structure [11, 12]

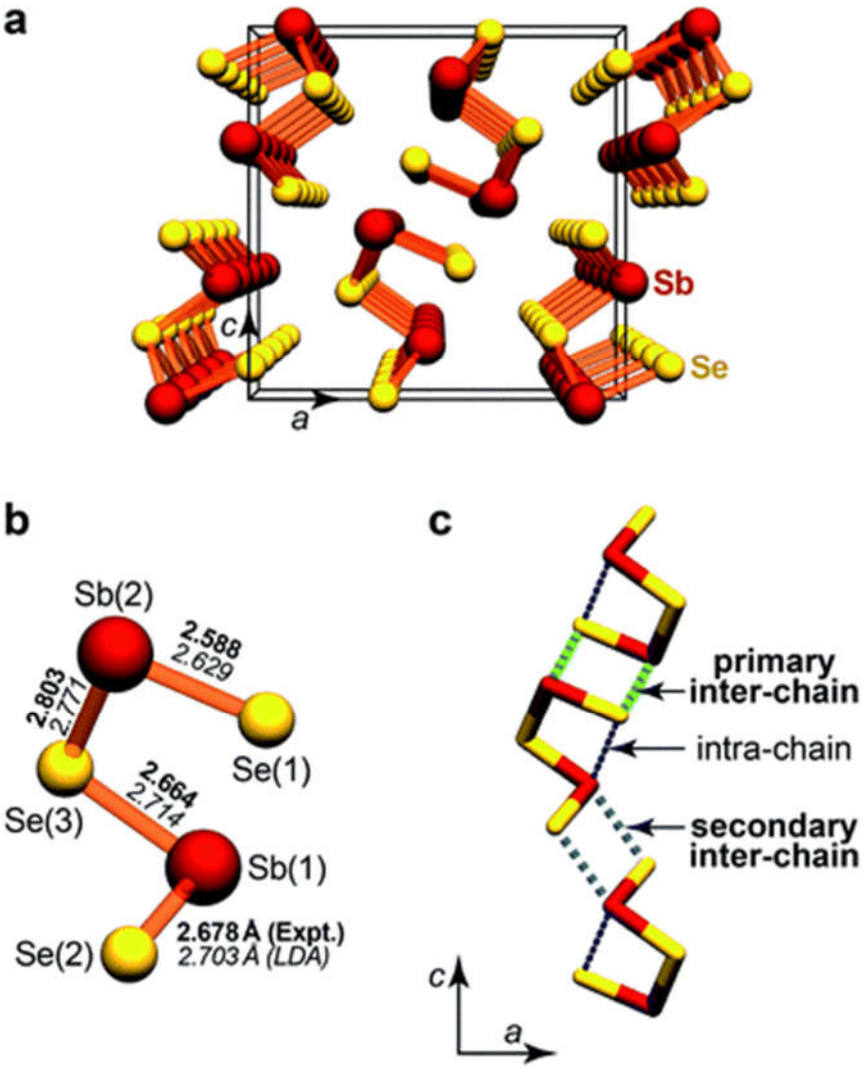

Figure 2 - (a) View in the short b - axis. (b) Fragment from a with labels. (c) Structural Drawing showing the weak c - axis contact [12].

1.2. Sb_2Se_3 Thin film deposition techniques.

Different chemical methods mainly represented by Chemical Bath deposition, Photo-electro deposition, Hydrothermal deposition, Microwave-Stimulated Solvothermal deposition and physical methods such as Thermal Evaporation, Co-Evaporation, Closed Space Sublimation, E-beam Evaporation, Pulsed laser Ablation and Magnetron Sputtering deposition have been used for the fabrication of Sb_2Se_3 films. The film properties have been strongly depended on the deposition method and conditions applied.

1.2.1. Sb_2Se_3 Thin film by thermal evaporation and co-evaporation.

Thermal evaporation and co-evaporations belong to the family of physical techniques that utilize the solidification of material vapors on the substrate surface [13]. Most of physical deposition methods use stoichiometric Sb_2Se_3 materials as the main source.

Liu et al, investigated the influence of deposition temperature on properties of Sb_2Se_3 thin films thermally-evaporated onto FTO substrates [14]. As-grown films were amorphous when deposited at room temperature (RT) and 150^{o}C. The fast annealing performed for RT films at 290^{o}C during 10-20 min yielded the formation of crystalline materials consisting of orthorhombic Sb_2Se_3 and exhibiting the minimal surface roughness. However, the presence of some voids was detected. The roughness of the film deposited at 150^{o}C and then thermally-treated at 290^{o}C was higher compared to the RT films. The films grown at 290^{o}C were found to be crystalline, composed of large grains, free of pinholes and cracks, while the presence of nanorods could be clearly observed. The p-type conductivity and the direct transition type with the value of 1.2 eV are reported for Sb_2Se_3 films prepared at 290^{o}C [14].

Kamruzzaman et al. [15] compared the electronic and optical properties of Sb_2Se_3 thin films thermally-evaporated onto p-Si and glass substrates. The films deposited at RT exhibited a smooth surface with undefined grain size and were amorphous in nature. The optical transition type of Sb_2Se_3 reported is controversial. The bandgap values determined from UV-Vis spectra were postulated to be as 1.6 eV for direct transition and 1.0 eV for indirect transition, respectively.

The effect of substrate temperature on the properties of Sb_2Se_3 films fabricated by co-evaporation of Sb_2Se_3 and Se on Mo-coated soda lime glass substrates pre-treated in Se atmosphere has been studied in [16]. The substrate temperature was varied from 200^{o}C to 350^{o}C. Irrespective of the deposition temperature employed, all the Sb_2Se_3 films were compact, crystalline and composed of orthorhombic

Sb_2Se_3. Films deposited at temperatures of 200-330^oC exhibited the preferred orientation along the (221) plane. By increasing the deposition temperature from 330^oC to 350^oC, the intensity of the (221) peak weakened while the intensity of (120) peak become more intense. Higher substrate temperature favored larger grain size.

1.2.2. Sb_2Se_3 Thin film deposition by closed spaced sublimation.

Close-spaced sublimation (CSS) is a deposition method utilizing the transfer of vaporized species from material sources to the substrate. This method is widely used in PV industry to produce high-quality thin films at different atmospheres [17].

Li et al. [18], reported the deposition of compact, adhered, phase-pure Sb_2Se_3 films grown by CSS at 250^oC on Si substrates. The films were orientated along the (001) plane.

Two-step close spaced deposition on titanium oxide layers performed at a source temperature of 350^oC (seed layer) and then at a source temperature of 450^oC (main layer) yielded the formation of stoichiometric, tight-packed, uniform, and pinholes free Sb_2Se_3 films [19]. The film demonstrated preferred orientation along the (211) and (221) planes and showed high absorption coefficient of about 10^5 cm^{-1} and a direct bandgap value of ~1.2 eV [19].

The formation of CSS Sb_2Se_3 nanorods at substrate holder temperature of 270^oC on Mo-coated glass substrates pre-treated in Se atmosphere enabled to construct the record 9.2%-efficient core-shell structured antimony selenide nanorod array solar cell with a structure of glass/Mo/MoSe2/ Sb_2Se_3/TiO2/CdS/HR-ZnO/LR-ZnO/Ag [20].

1.2.3. Magnetron sputtering.

Magnetron Sputtering is a physical deposition method, in which the material to be grown is bombarded with glow discharge-assisted high energy ions. The generated atoms of desired materials pass through the discharged region and form films on the targeted surface [21]. Among the other methods used for the film deposition in many application areas, Magnetron Sputtering could provide undeniable advantages such as simplicity and high depositing rates, and capability to deposit uniform and highly-adherent to various metallic, alloying and other compound films having different functional properties [21-23]. Figure 3 represents a schematic diagram for the magnetron sputtering system.

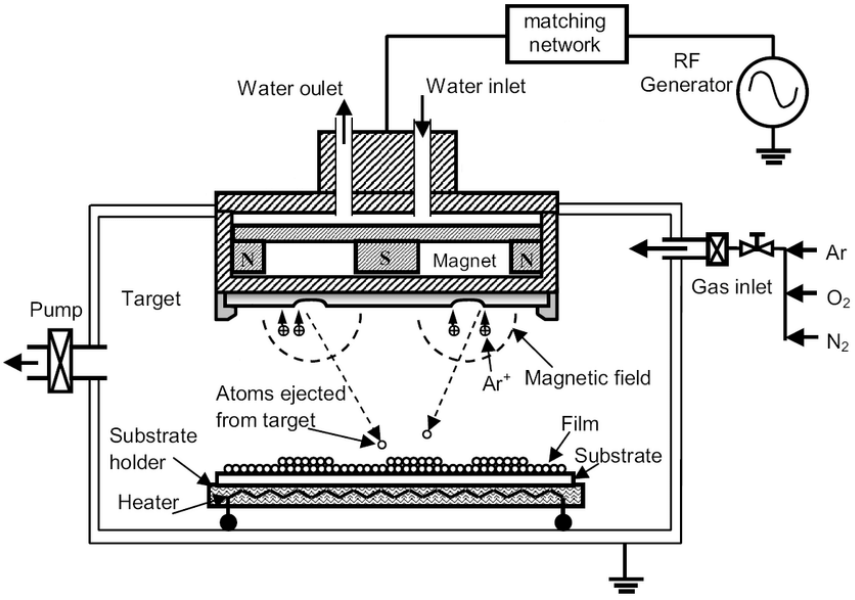

Figure 3 - Schematic representation of the magnetron sputtering system [24].

1.2.4. Sb_2Se_3 Thin films by magnetron sputtering.

Liang et al. [25], investigated the effect of the substrate temperature varying from RT to 400°C on the properties of Sb_2Se_3 thin films grown on Mo-coated glass substrates. Films grown at temperatures below 200 °C were amorphous and flat, while those deposited at temperatures ≥ 250°C were crystalline, rougher and composed of the orthorhombic Sb_2Se_3 phase. Films grown at 325°C showed compact grain structure. Further increase in substrate temperatures to 375°C promoted the formation of highly uniform layers with monodispersed Sb_2Se_3 nanorods. In general, with increasing the deposition temperature from 250 to 350°C, selenium content decreased, direct bandgap values increased from 1.1 eV to 1.5 eV and crystallite size increased also.

Very similar results on the influence of substrate temperatures on structural and elemental composition properties of magnetron sputtered Sb_2Se_3 thin films have been reported in [26]. However, Chen et al. reported oppositely about decreasing the bandgap values from 1.6 eV to 1.2 eV when the substrate temperature increased from 200 to 325°C [26].

The effect of the deposition pressure on properties of Sb_2Se_3 thin films sputtered on FTO-covered glass substrates have been studied by Liang et al. [27]. Fast annealing in Vacuum for 5 min resulted in the

formation of crystalline Sb_2Se_3 films with the preferred orientation along the (211) and (221) planes. It has been reported that all films were selenium deficient regardless of deposition pressure employed, and the photo-current increased with the increasing deposition pressure.

In summary, it could be concluded that films deposited by the listed above physical methods at temperatures below 200°C are mostly amorphous with small grain sizes [15, 25, 28]. An increase in the substrate temperature resulted in orthorhombic Sb_2Se_3 films with better crystallinity and higher grain sizes [15, 16, 19, 25, 28 - 31]. Some authors reported the formation growth of Sb_2Se_3 nanorods when layers are grown at substrate temperatures above 300°C [20, 25, 28]. An increase in the deposition temperature intensified selenium deficiency in Sb_2Se_3 films [29, 25, 28]. Optical properties of Sb_2Se_3 films grown by the listed above physical deposition methods have been found to depend on the experimental protocol employed the absorption coefficient has been reported to be ~10^5 cm^{-1}, direct optical bandgap values varied from 1.2 eV to 1.6 eV [15, 30, 31].

1.3. Post deposition treatment

Leng et al. [32] investigated the effect of post deposition selenization on properties of Sb_2Se_3 thin films and solar cell performance. Sb_2Se_3 thin films were thermally evaporated on CdS layers and then selenized in the same chamber. A solar cell configuration glass/FTO/CdS/ Sb_2Se_3/Au was used. Selenization was performed for 30 minutes at different temperatures fixed as; 170°C, 200°C and 230°C. It has been reported that selenization at 200°C enabled to reach higher cell efficiency compared to as-deposited Sb_2Se_3 films, of 3.7% and 2.6%, respectively. Furthermore, selenization performed at 200°C for Sb_2Se_3 films resulted in better device parameters then those observed for samples selenized at 170°C and 230°C. All selenized films behaved better in the solar cell when compared with as-deposited layers. Film selenized at 230°C exhibited decreased cell performance than those produced at 200°C as re-evaporation of Sb_2Se_3 could have happened.

Liu et al [33], studied the influence of defects present in Sb_2Se_3 thermally-evaporated onto glass/ITO/CdS substrates at 290°C and then annealed in vacuum and selenium atmospheres on solar cell performance. First, the intrinsic defects were estimated by first principle calculations and it has revealed the presence

of cation–anion antisites as dominant defects in Sb_2Se_3. It has been shown that selenization decreased the presence of Sb_2O_3 and selenium deficiency in films, increased the grain size, improved p-type conductivity and carrier lifetime, and thus, improved the solar cell performance from 2.92% to 5.46% [33].

Tang et al [28], investigated the effect of post deposition selenization temperature on properties of magnetron-sputtered Sb_2Se_3 thin films and solar cell performance. They deposited Sb_2Se_3 thin films at RT on Mo-glass substrates and then annealed in selenium atmosphere at temperatures of 350^{o}C, 400^{o}C and 450^{o}C. It has been reported that as-deposited films have smaller grains than samples annealed at 350^{o}C. Annealing at 400^{o}C led to the formation of nanorod Sb_2Se_3 samples, micro voids were detected in the films. Annealing at 450^{o}C resulted in samples with reduced grain size and the presence of voids. Stoichiometric Sb_2Se_3 films were obtained when films were selenized at 350^{o}C, while those layers annealed at 400^{o}C and 450^{o}C were selenium rich. The solar cell with a configuration of Mo/Sb_2Se_3/CdS/ITO/Ag based on the layer annealed at 350^{o}C showed the cell parameters as 2.1% conversion efficiency of 2.1%, Voc of 0.343V, J_{sc} of 16.79 mAcm^{-2} and fill factor of 35.3%.

Shongalova et al, [34] investigated the influence of post deposition annealing in Hydrogen Selenide (H_2Se) on properties of Sb_2Se_3 thin films and cell performance. They started by first depositing thin films of Sb_2Se_3 using magnetron sputtering technique on three different substrates (Glass, Glass-Mo and p-type Silicon). This was then followed by annealing each of the substrate type in H_2Se flow at 300^{o}C, 350^{o}C and 400^{o}C for 900 seconds each. When checked for change in selenium-antimony composition, it was reported that: for films on glass only substrate, there was an excess of selenium at the three annealing temperatures with 350^{o}C having the highest amount; similar result was reported for films on glass-Mo substrate; for films deposited on Silicon substrate, the ratio was almost stoichiometry with just a little more selenium. It was also reported that the films experienced increase in grain size from as deposited to 300^{o}C and are biggest at 400^{o}C for all three substrate types. From XRD, it was reported that the same peaks (of 201, 301, 302 and 402) were observed for all substrate types and temperature, however, there were additional peaks on the Mo substrate showing the presence of Sb and $MoSe_2$. For electrical characterization: free hole concentration increased from that at annealing temperature of 300^{o}C to a maximum at 350^{o}C and then reduced at 400^{o}C; mobility was almost same at 300^{o}C and at 400^{o}C it then reduced to a minimum at annealing temperature of 350^{o}C; resistivity was highest at 300^{o}C and then reduced by one order at 350^{o}C and then to a minimum at 400^{o}C. photoluminescence performed on the Si substrate showed broad band of approximately 0.85eV at annealing temperatures 300 and 350^{o}C and approximately 0.75eV at annealing

temperature of 400°C. Overall, they concluded that the holes and acceptors concentrations are low and the film would need some doping.

Kamruzzaman et al. [15] reported the formation of Sb_2Se_3 layers with improved grain size and absorption coefficient to be greater than 10^5 cm^{-1} after annealing in flowing Nitrogen at 290°C for 30 min.

To summarize, post-deposition thermal treatment in selenium containing atmosphere has improved the grain size, elemental composition to more stoichiometric composition, decreased the presence of oxygen containing phases, improved the electrical properties and as a result improved solar cell parameter [15, 32, 33, 28, 34].

1.4. Application of Sb_2Se_3 films

Orthorhombic Sb_2Se_3 is a non-toxic material consisting of easy-available elements. [11]. In addition to the material non-toxicity, Sb_2Se_3 exhibits optical properties such as direct bandgap values in the range of 1.0–1.5eV and indirect values varying in the region of 1.0– 1.22eV depending on experimental procedures, the absorption coefficient of above 10^4 cm^{-1} , and electrical properties such as hole conductivity of about 10^{-7} $\Omega^{-1}cm^{-1}$, electron mobility of 15 cm^2/Vs and hole mobility of 42 cm^2/Vs recorded at room temperature [11, 35-37]. Thus, notable physical properties make antimony (III) selenide appealing for different applications such as thin-film solar cells [20], thermoelectric cooling devices [38, 39] and lithium-ion batteries [40].

Recently, Sb_2Se_3 has garnered significant research interest as an attractive absorber material for cost-effective thin-film solar cells to replace layers containing non-abundant and/or toxic elements such as In, Ga, Te and Cd. The solar cells with the layer obtained by co-evaporation of Sb_2Se_3 and Se in the substrate configuration of Ag/ITO/ZnO/CdS/ Sb_2Se_3/Mo/Glass showed a conversion efficiency of 4.25% [16]. It has been demonstrated that solar cells based on CSS Sb_2Se_3 nanorods acting as absorber and CdS buffer layers have reached the record device efficiency of 9.2% [20].

1.5. Summary and aim of study

Thin films of Sb_2Se_3 photo absorbers can be fabricated by different deposition techniques, post deposition treatment in Nitrogen and Se-containing atmospheres has been reported. There are few studies on the fabrication of Sb_2Se_3 films using the magnetron sputtering deposition technique, which has a great potential to produce uniform and well-adhered films with controlled impurities content. In the literature, there is still a lack of knowledge on post-deposition treatment suitable for Sb_2Se_3 thin films. Considering the listed above aspects, the present investigation is aimed at:

- To investigate the influence of deposition temperatures on properties of Sb_2Se_3 thin films deposited by RF Magnetron Sputtering deposition technique.
- To study the influence of post-deposition thermal treatment in Ar-Se atmosphere on the properties of sputtered Sb_2Se_3 thin films.

CHAPTER TWO: EXPERIMENTAL SECTION

2.1. Substrate preparation

The major substrate preparation process is the substrate cleaning, it is an integral part of thin film deposition. The substrate surface contains some impurities which if not removed prior to deposition will affect the quality of the deposition as well as properties of the film. [41, 42].

Two types of substrates were used for Sb_2Se_3 thin films deposition; the soda lime glass, and Mo-coated soda lime-glass substrates. The Soda lime glass substrates were first cleaned in concentrated sulfuric acid for 15 minutes at 50^oC, then washed with de-ionized water, and then cleaned in an ultrasonic bath for another 15 minutes, and was followed by rinsing with de-ionized water and drying with nitrogen gas. After drying the cleaned glass was then placed in the UV-Ozone cleaner for another 15 minutes to complete the cleaning process.

A plasma cleaner was used to clean the Mo coated glass substrates for 15 minutes prior to deposition.

2.2. Antimony selenide deposition

The thin films of Sb_2Se_3 were produced using RF Magnetron sputtering technique provided by the Angstrom Engineering Evovac 030 three sputter sources with glow discharge. A 4 inch 99.99% pure Sb_2Se_3 target (Tesbourn Ltd, London) was used as the source of deposition, this was placed in the source position of the sputtering chamber, with the soda lime glass and Mo-coated glass set in the substrate holder. The distance between the target and substrates was maintained at 20cm, all substrates were rotated at 5rev/min during deposition.

The Sb_2Se_3 thin films were sputtered at substrate temperatures: RT, 200^oC, and 300^oC. Before depositions, the chamber was pumped down to about 10^{-7}Torr. High purity (99.999%) argon plasma (working pressure 20mTorr) was used during the sputtering process. The applied power density of 1.3watt/cm^2 lead to the deposition rate of 3Å/s. The thickness of the films was 1µm and was adjusted by the use of oscillatory quartz crystal microbalance, and was confirmed by SEM measurements.

Preliminary investigations were done to determine the best combination of sputtering parameters; argon pressure, applied power density, deposition rate, substrates holder rotational speed, and chamber

pressure. The combination of parameters we settled for enabled the fabrication of film with similar morphology on the SLG and Mo coated SLG

2.3. Post deposition heat-treatment

The as-deposited Sb_2Se_3 thin films were annealed with elemental selenium and filled by Ar (100Torr) at temperature range 300-400^oC in isothermal sealed quartz ampoules. The duration of selenization was 30min. At the end of thermal treatments, samples were pulled out and cooled down to room temperature.

2.4. Methods of sample characterization.

As-deposited and annealed Sb_2Se_3 thin films were analyzed using different characterization techniques to study the transformation that happened in the investigated films. Morphology, the elemental and phase composition, optical and electrical properties were investigated.

2.4.1. Scanning electron microscopy.

The evolution of the surface morphology and the film thickness of the studied thin films were analyzed by the high-resolution scanning electron microscope (HR-SEM) Zeiss Merlin equipped with In-Lens secondary electron detector for topographic imaging. The samples were investigated at low excitation voltage that allows to avoid charging of samples. The measurement was made at operation voltage in the range 1.5-2eV and the probe current of 160pA.

The scanning electron microscope (SEM) permits to obtain three-dimensional topographic images of the surfaces in a wide magnification range. In the SEM, the sample is examined with a focused electron beam moving across the sample to form an image. The interaction of the electron beam with the surface of sample results in different signals: backscattered electrons, secondary electrons, characteristics X-rays [43]. Low energies secondary electrons are generated near the surface and provides the fine-scale topological information of the studied samples. Backscattered electrons produced as a result of elastic

collision with atoms of the sample provides the atomic number or orientation information. The analysis of characteristic X-rays gives chemical information about the investigated material [44, 45].

2.4.2. Energy dispersive X-ray spectroscopy

The chemical composition of the thin films was determined using an energy dispersive x-ray analysis (EDS) system (Bruker EDX-XFlash6/30 detector). Operating voltage of 20KV was used for all measurement and the concentrations of elements were calculated by using PB-ZAF standard less mode.

2.4.3. X-ray diffraction.

X-ray diffraction (XRD) analysis using a Rigaku Ultima IV diffractometer with CuKα radiation (λ = 0.154nm, at 40kV and 40mA) in Bragg Brentano geometry, was used to investigate the crystalline structure of the films. The XRD peaks were identified using JCPDS files. The lattice constants and crystallite sizes were calculated by Rigaku PDXL software.

The analysis is based on the constructive interference of monochromatic radiations and the sample, the x-rays are concentrated on the sample, the incident rays going through the sample creates interference and diffracted rays. The diffraction pattern generated gives a unique fingerprint of the crystals in the sample, this can then be compared with the standard reference patterns to identify the actual crystal present in the sample [46].

The Scherrer equation was used to determine the crystallite size of our films [47]

$$B(2\theta) = \frac{K\lambda}{Lcos\theta} \tag{3.1}$$

Where L is the average crystalline size, K is a dimensionless shape factor with values from 0.62 to 2.08, B(2θ) is the full width at half-maximum (FWHM) of preferred peak in radians, θ is the Bragg angle and λ is the X-ray wavelength (0.154nm) [47-49].

To determine the interplanar spacing of the diffraction pattern we used the Bragg's law provided by Cullity and Stock [50] as:

$$n\lambda = 2d\ sin\theta \tag{3.2}$$

Where d represents the interplanar spacing and n, the order of diffraction is equal to 1. Because the Sb_2Se_3 films showed orthorhombic structure, we used the d spacing formula for orthorhombic given by Cullity and Stock [50] to determine the lattice constants a, b and c:

$$\frac{1}{d^2} = \frac{^2}{a^2} + \frac{k^2}{b^2} + \frac{l^2}{c^2} \quad (3.3)$$

Where h, k and l are the Miller indices [50].

2.4.4. Raman spectroscopy

The room temperature Raman spectra were recorded by using Horiba LabRam HR spectrometer with green laser (λ = 532nm) as an excitation source. The incident laser light was focused on the surface of the sample within a spot of 1μm. The spectral resolution of the spectrometer was about 0.5cm^{-1}.

Raman spectroscopy is a spectroscopic technique that helps with sample identification using information from molecular vibration. For measurements, a monochromatic light source is directed towards the sample, a detector reads the scattered light, majority of which are of same frequency as the incident while the remaining few are of a different frequency (caused by interactions between the incident electromagnetic waves and vibrational energy level of the sample). The Raman shift which is the energy difference between the incident and the scattered lights is used to identity the phase composition of the samples [51, 52].

2.4.5. Ultraviolet-visible spectroscopy.

The total optical transmittance and reflectance spectra were measured using the Agilent Cary5000 UV-VIS-NIR spectrophotometer in the wavelength range of 300 – 1500nm for as deposited and annealed samples on soda lime glass substrates.

The operating principle involves the sample being illuminated by an electromagnetic radiation source, part of this radiation that is transmitted, reflected or absorbed are then analyzed as with respect to the incident radiation. From the spectrophotometer we obtained the value of Reflectance (R) and

Transmittance (T), these values are then used in the equation provided by Saini et al [53] to determine the absorption coefficient (α):

$$\alpha = \frac{\ln\left[\frac{(1 \quad R)}{T}\right]}{t} \tag{3.4}$$

Where t = film thickness. To determine the bandgap, the Tauc's formula was utilized [53 - 55].

$$(\alpha \ \ v) = A\big(\ \ v \quad E_g\big)^n \tag{3.5}$$

Where A is a constant of proportionality, E_g is the energy band gap and n denote the nature of transition. For allowed direct transition, n = ½, and the band gap can be extrapolated from the graph of $(\alpha hv)^2$ versus hv, while for allowed indirect transition, n = 2 and band gap can be gotten from the graph of $(\alpha hv)^{1/2}$ versus hv [54 - 56].

2.4.6. Scanning kelvin probe.

Surface potential changes for the as-deposited and annealed Sb_2Se_3 films were measured by scanning Kelvin probe system (SKP5050) equipped with 2mm gold-covered vibrating tip and under pulsed laser irradiation (670nm, 20mW/cm^2 intensity) [57].

Kelvin probe Technology was used to measure the change in work function of the films surfaces under light and in the dark, this gives information about the photo sensitivity of the films. The technique uses a non-contact and non-destructive method to measure the change in potential difference between the tip of a vibrating metal and the surface of the measured sample, both forming a capacitor (vibrating capacitor) [58].

2.4.7. Electrical properties.

Hot point probe method was used to determine the type of conductivity the films possess.

Two probe Van der Pauw with indium contact was also used to determine the resistivity of the films.

2.5. Solar cell.

Our best film was made into a solar cell, CdS buffer were deposited by chemical bath depsosition method onto the developed Sb_2Se_3 film to prepare the solar cell with structure: graphite/ZnO:Al/i-ZnO/CdS/Sb_2Se_3/Mo. i-ZnO and front contact ZnO:Al were deposited by magnetron sputtering, and the graphite paste was used to improve the electrical contact with the ZnO:Al layer. The cell performance was measured using a solar simulator with light intensity of 100mW/cm^2. The parameters that determines that helps to measure the cell performance; fill factor (FF) and cell conversion efficiency are related by the equations [59]:

$$\text{Fill Factor, } FF = \frac{I_{max} X V_{max}}{I_{SC} X V_{OC}} \quad (3.6)$$

Where, I_{max} is the maximum output of current (A)

V_{max} is the maximum output of voltage (V)

I_{SC} is the short circuit current (A)

And V_{OC} is the open circuit voltage (V).

$$\text{Cell conversion efficiency, } \eta = \frac{I_{SC} X V_{OC} X FF}{P_{in}} \quad (3.7)$$

Where, P_{in} is the intensity of incident light (W).

CHAPTER THREE: RESULTS AND DISCUSSION

3.1. As-deposited films.

3.1.1. Composition and morphology.

The EDX and HR-SEM techniques were employed to investigate the elemental composition and morphology of films, respectively. Irrespective of the substrate temperature employed, EDX studies revealed films with a composition of 42 at. % antimony to 58 at. % selenium which are selenium deficient compared to a nearly stoichiometric composition of 40 at. % antimony to 60 at. % selenium for all as-deposited films. Figure 4 compares the morphologies and cross-sectional views of films grown at RT, 200 and 300°C. It could be clearly seen that all the films exhibited homogenous coverage without cracks and holes (Figure 4). According to SEM images, films grown at RT and 200°C were amorphous and consisted of small grains, while those grown at 300°C were crystalline and consisted of large grains.

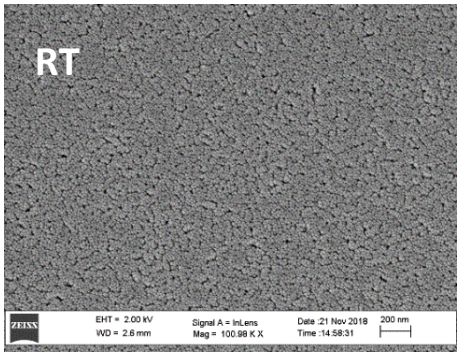

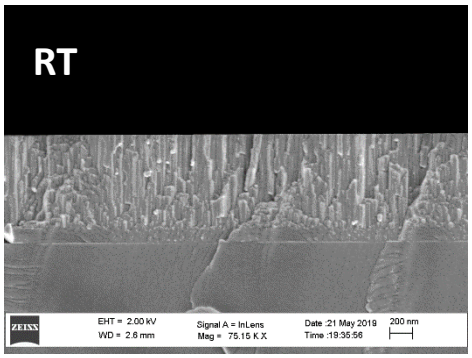

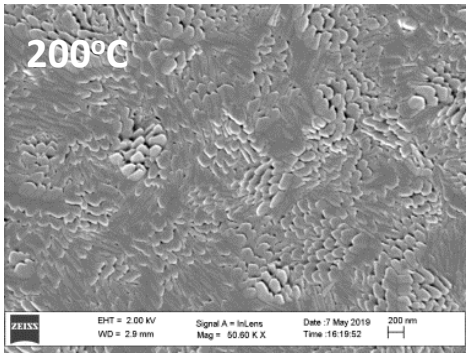

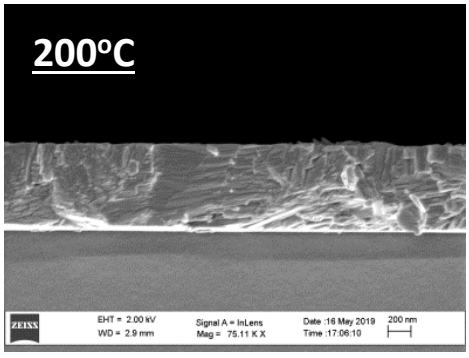

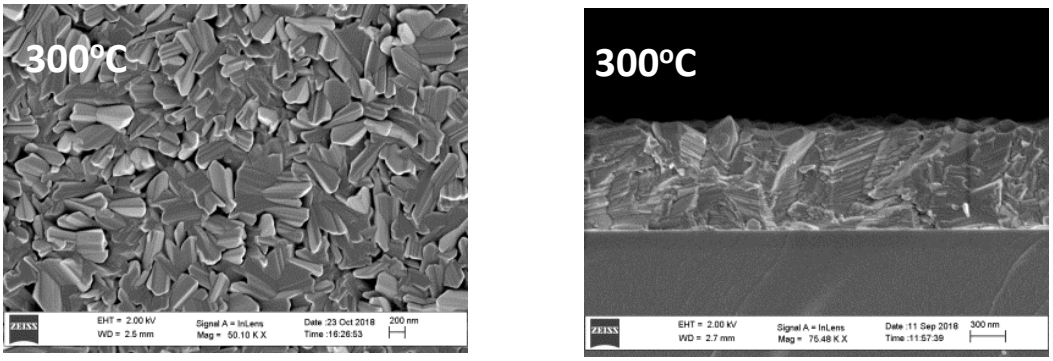

Figure 4 - HR-SEM surface and cross section images of Sb_2Se_3 films deposited at temperatures; RT (top), 200°C (middle) and 300°C (bottom).

3.1.2. Structural analysis.

The structural properties of sputtered Sb_2Se_3 films were studied by means of X-ray diffractometry (XRD) and Raman spectroscopy. Figure 5a presents XRD patterns of films grown at RT, 200 and 300 °C. XRD studies revealed that RT films are amorphous as the diffractogram shows no XRD peaks. The films deposited at 200 and 300°C are crystalline and consisted of the orthorhombic Sb_2Se_3 phase (PDF 01-089-0821) [10].

With an increase in substrate temperature, the XRD peaks become tight and their intensities increased. This fact can be associated with an increase in crystallite sizes (See Table 1) and it is a quite typical characteristic for physical deposition methods [14 - 16, 19, 25, 26, 28 – 31, 60, 61]. By increasing the substrate temperature from 200 to 300 °C, the lattice parameters also decreased to the values of bulk material, indicating the formation of more relaxed structure.

By the detailed contrasting of XRD patterns (Figure 5a) and the powder reference for orthorhombic Sb_2Se_3 (PDF 01-089-0821), the crystallites in sputtered Sb_2Se_3 films deposited at 200 °C and 300 °C seemed to exhibit a preferred growth. The Sb_2Se_3 films deposited at 200 °C and 300 °C displayed the most intense diffraction peak along the (200) and (061) planes, respectively, while the (221) diffraction peak was the most intensive peak for Sb_2Se_3 powder. The ratios of peak intensities (I (200)/I (221) or I (061)/I (221)) were 8.5 and 57.1 for Sb_2Se_3 films sputtered at 200 and 300 °C, respectively. As ratios of I(200)/I(221) or I(061)/I(221) peak intensities for powder were below 0.1 in both cases, thus the film grown at 200°C had a preferred orientation along the (200) plane and the film grown at 300°C had a preferred orientation along the (061) plane parallel to the substrate.

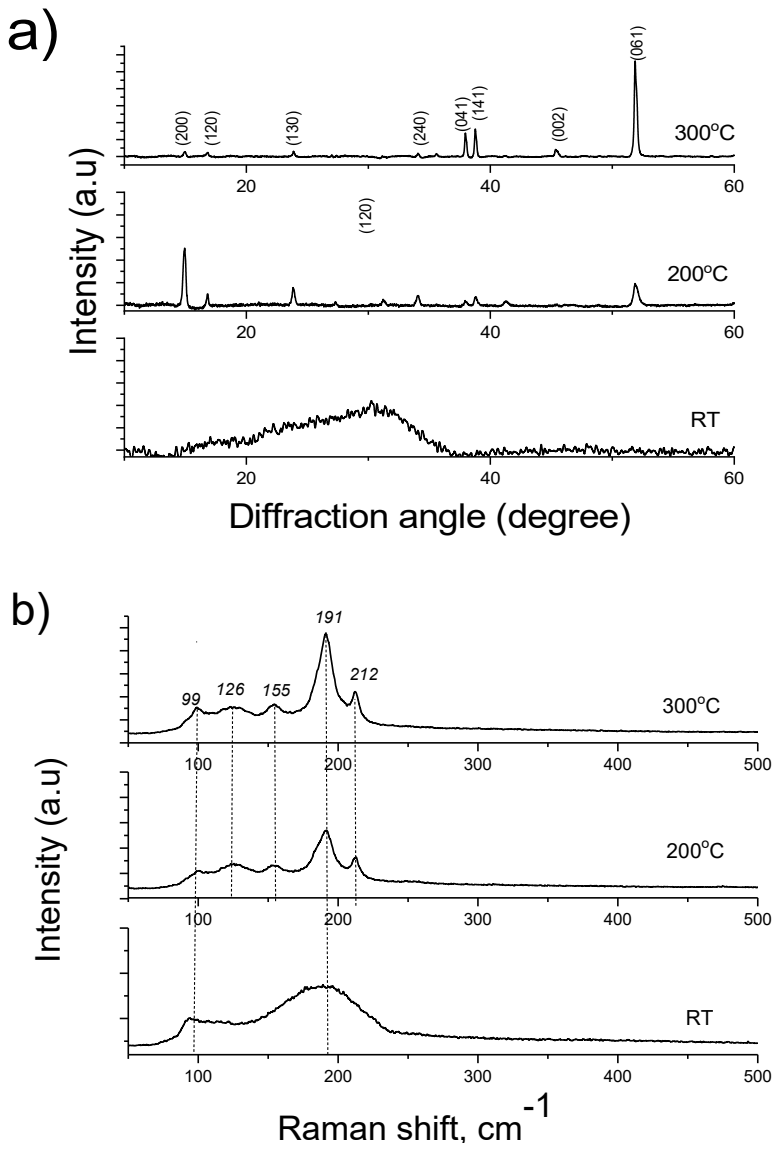

Figure 5. (a) XRD patterns and (b) Raman spectra of Sb_2Se_3 films deposited at RT, 200 and 300°C.

Table 1 - The structural parameters and optical bandgap values (Eg) of Sb_2Se_3 films deposited at RT, 200 and 300°C.

Sample	**Crystallite size (nm)**	**Lattice parameters**			E_g (eV)
		a(Å)	b(Å)	c(Å)	
As-deposited at RT					1.75
As deposited at 200C	20	11.722	11.756	3.992	1.50
As deposited at 300C	56	11.702	11,773	3.982	1.25

The Raman spectra of as-deposited films deposited at various substrate temperatures are presented in Figure 5b. The films deposited at 200 and 300 ^{o}C exhibited the Raman spectra with higher resolution compared to RT films, as more crystalline films formed at those temperatures. Raman spectra of films deposited at 200 ^{o}C or 300 ^{o}C are similar, displaying the peak positions at 99 cm^{-1}, 126 cm^{-1}, 155 cm^{-1}, 191 cm^{-1}, and 212 cm^{-1}, characteristics of Sb_2Se_3 [62 - 65]. The Raman results correlate with those obtained from the XRD studies.

3.1.3. Optical properties.

The optical bandgap values of as-deposited Sb_2Se_3 films were estimated based on UV–Vis data employing the formula 3.5 known as the Tauc relation [54 - 56], and shown in Figure 6. As evident from Table 1, RT deposition led to the formation of films with E_g value of 1.75 eV. Such high bandgap values can be associated with an amorphous material structure and very small grain size (Table 1). With an increase in the substrate temperature, the bandgap values decreased in accordance with increasing the crystallite size in films. For instance, films deposited at 200 ^{o}C showed the bandgap value of 1.5 eV, while those grown at 300 ^{o}C displayed 1.25 eV. Our results are in good agreement with the bandgap values reported for sputtered Sb_2Se_3 films [25 - 27].

To summarize, our studies on as-deposited films clearly demonstrated than crystalline Sb_2Se_3 films with higher crystallite size, lattice parameters and optical bandgaps close to the bulk values can be grown at 300 ^{o}C. However, these films are selenium deficient. To compensate the selenium deficiency in films and to produce more stoichiometric materials, the post-deposition thermal treatment in Ar-Se atmosphere were further employed.

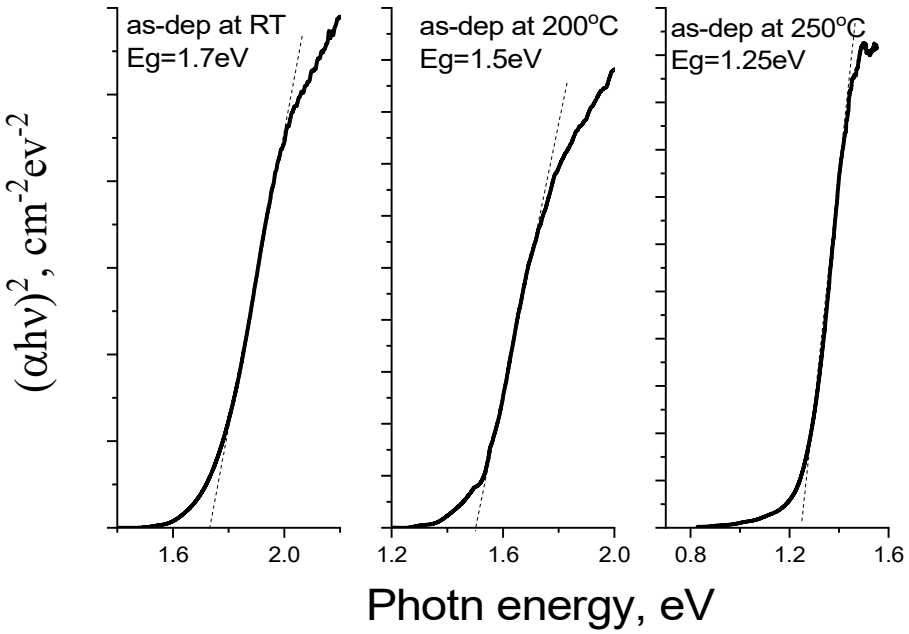

Figure 6 - Tauc plots of as-deposited Sb_2Se_3 films at RT, 200 and 300°C.

3.2. Sb_2Se_3 films annealed in Ar-Se atmosphere.

3.2.1. Composition and morphology.

To increase the selenium content in sputtered Sb_2Se_3 films, films deposited at 300°C were thermally-treated in an atmosphere containing selenium and argon at annealing temperatures varying from 300 to 400°C. The EDX results revealed that all annealed films have a nearly stoichiometric composition of 40 at. % antimony to 60 at. % selenium regardless of annealing temperature employed. Figure 8 contrasts the morphological properties of as-deposited Sb_2Se_3 films grown at 300°C on Mo-covered glass substrates and those of annealed in Se-containing atmosphere at 300, 350, and 400°C. Annealing in Ar-Se atmosphere at 300°C yields the formation of denser and compact structure with larger and rounded grains compared to as-deposited films (Figure 7). Similar morphology is observed for the films annealed at 350°C. Annealing at 400°C lead to films with further increased grain size, while some holes between grains could be detected (Figure 7).

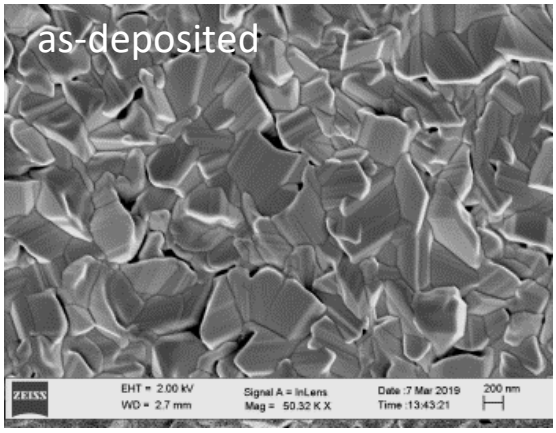
as-deposited
EHT = 2.00 kV
WD = 2.7 mm
Signal A = InLens
Mag = 50.32 K X
Date :7 Mar 2019
Time :13:43:21
200 nm

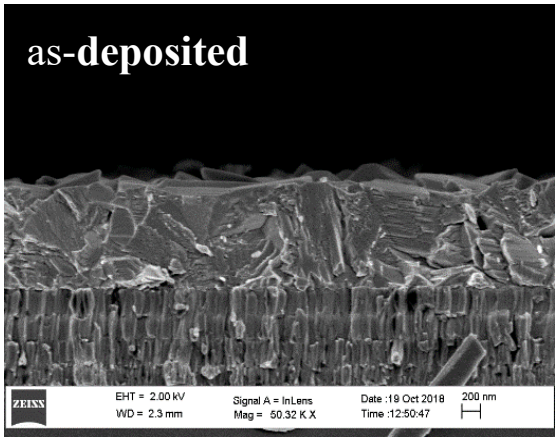
as-deposited
EHT = 2.00 kV
WD = 2.3 mm
Signal A = InLens
Mag = 50.32 K X
Date :19 Oct 2018
Time :12:50:47
200 nm

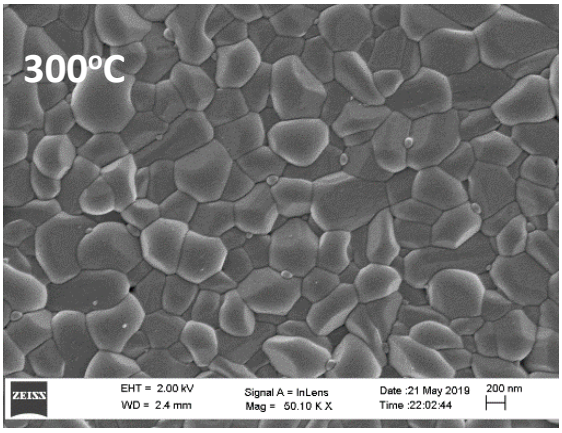
300°C
EHT = 2.00 kV
WD = 2.4 mm
Signal A = InLens
Mag = 50.10 K X
Date :21 May 2019
Time :22:02:44
200 nm

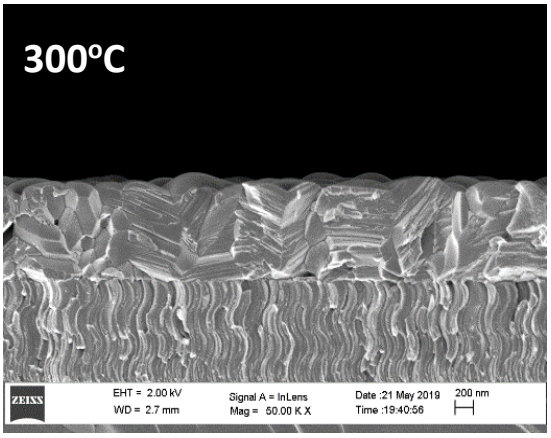
300°C
EHT = 2.00 kV
WD = 2.7 mm
Signal A = InLens
Mag = 50.00 K X
Date :21 May 2019
Time :19:40:56
200 nm

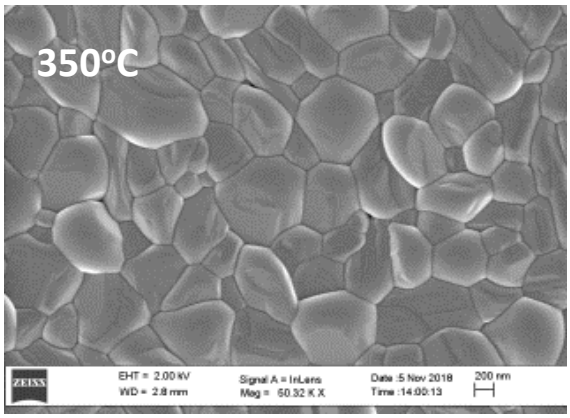
350°C
EHT = 2.00 kV
WD = 2.8 mm
Signal A = InLens
Mag = 50.32 K X
Date :5 Nov 2018
Time :14:00:13
200 nm

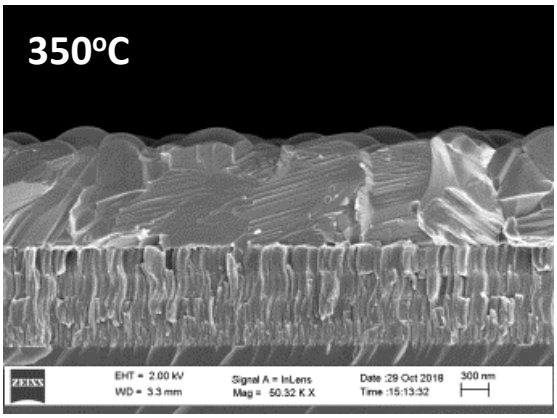
350°C
EHT = 2.00 kV
WD = 3.3 mm
Signal A = InLens
Mag = 50.32 K X
Date :29 Oct 2018
Time :15:13:32
300 nm

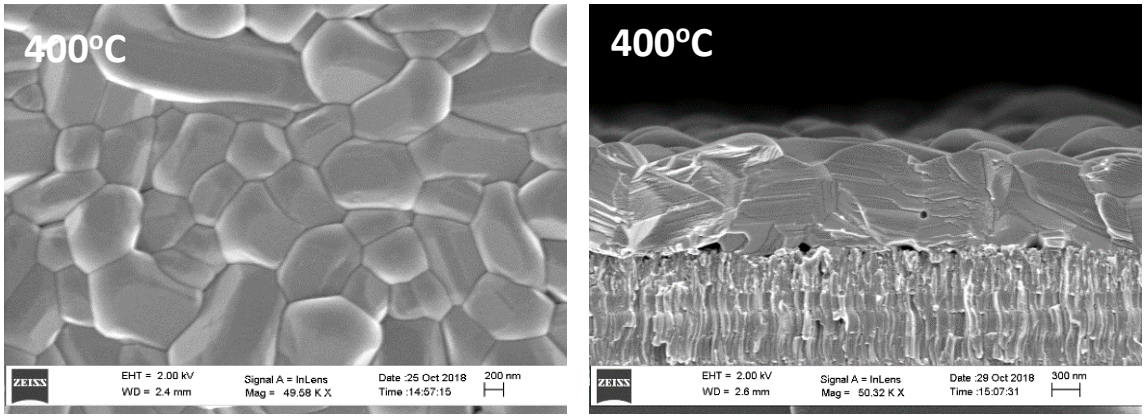

Figure 7 - HR-SEM images of Sb_2Se_3 films deposited onto Mo-covered substrate at 300°C and those of annealed in Ar-Se atmosphere at 300, 350 and 400°C substrate temperatures.

3.2.2. Structural analysis.

Figure 8a demonstrates diffractograms of as-deposited films grown at 300°C and those of annealed in Ar-Se atmosphere at 300 and 350°C. Diffractograms of films annealed at 400°C were very similar to those recorded for films annealed at 350°C and not presented here. All the films annealed in Ar-Se atmosphere were consisted of the orthorhombic Sb_2Se_3 phase (PDF 01-089-0821) [10] and exhibited the preferred orientation along the (061) plane. With an increase in annealing temperature, a gradual increase in crystallite size from 56 nm to 80 nm is observed. The Raman spectra of as-deposited Sb_2Se_3 film grown at 300°C and those of annealed in Ar-Se atmosphere are shown in figure 8b. All Raman spectra of annealed films are similar and similar to as-deposited films, showing the peaks at 99cm^{-1}, 126cm^{-1}, 155cm^{-1}, 191cm^{-1}, and 212cm^{-1}, characteristics of Sb_2Se_3 [62 - 65].

The main peaks at around 189 cm^{-1} and 210cm^{-1} are linked to the heteropolar Sb-Se bond vibrations present in the $SbSe_{3/2\text{-pyramides}}$ (Sb_2Se_3 basic structural unit), the gentle peak at about 151cm^{-1} is linked to Sb-Sb bond in Se_2Sb – $SbSe_2$ structural unit, the mild peak at about 120cm^{-1} corresponds to the Se-Se bonds, and the band at about 98cm^{-1} corresponds to the Se_6 rings with the rhombohedral structure [62 - 65]. The Raman results correlate with those obtained from the XRD studies.

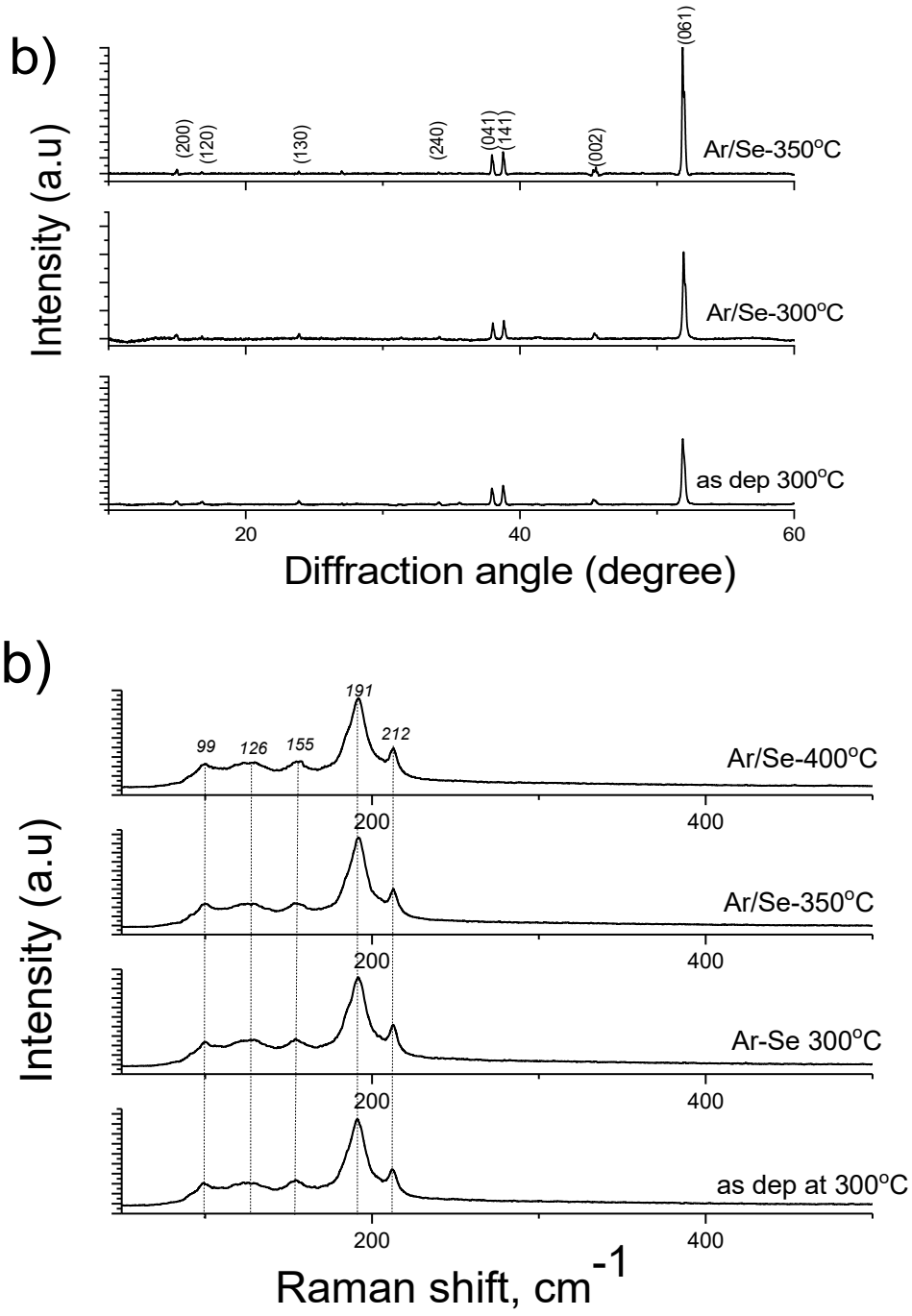

Figure 8 - (a) XRD patterns and (b) Raman spectra of Sb_2Se_3 films deposited at 300°C and those of annealed in Ar-Se atmosphere at 300, 350 and 450°C.

3.2.3. Optical Studies.

The absorption coefficient for all films was calculated as explained in section 2.4 of this report using the equation 3.4. The absorption coefficient values were found to be above 10^4 cm^{-1}. The optical bandgap values of Sb_2Se_3 films annealed at 300, 350 and 400°C in Ar-Se atmosphere were estimated using the UV–Vis absorption spectra and employing the formula 3.5 known as the Tauc relation [54 - 56]. Figure 9 presents the Tauc plots of as-deposited Sb_2Se_3 grown at 300°C and those of annealed Sb_2Se_3 films at 300, 350 and 400°C. As-deposited Sb_2Se_3 films exhibits the bandgap value of 1.25 eV. With an increase in the annealing temperature from 300 to 400°C, the optical bandgap values decreased from 1.25 eV to 1.17 eV in accordance with increasing the crystallite size from 56 nm to 80 nm. Our results are in good agreement with the literature data [25 - 27].

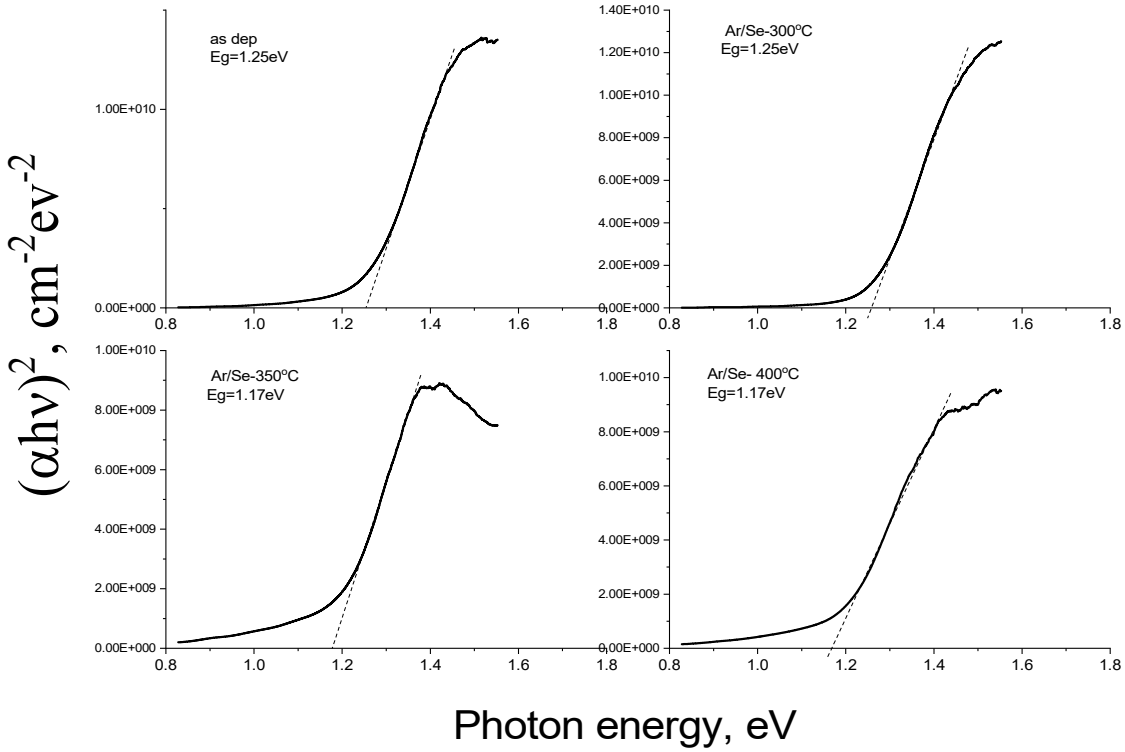

Figure 9 - Tauc plots of as-deposited Sb2Se3 films grown at 300°C and those of annealed in Ar-Se atmosphere at various substrate temperatures.

3.2.4. Surface Potential of films.

Kevin probe technique was used to determine the change in work function (WF) on the films surface in dark condition and under light, this difference tends to reveal the sensitivity of the films to light. Figure 10 shows the work function plot for the films annealed in Ar-Se atmosphere. The as deposited film (at 300°C substrate temperature) had the lowest change in work function of about 20mV, this value increased to about 60mV for the film annealed in Ar-Se at 300°C and increased to the maximum value of 80mV for the film annealed at temperature of 350°C but then dropped to about 70mV for the film annealed at 400°C.

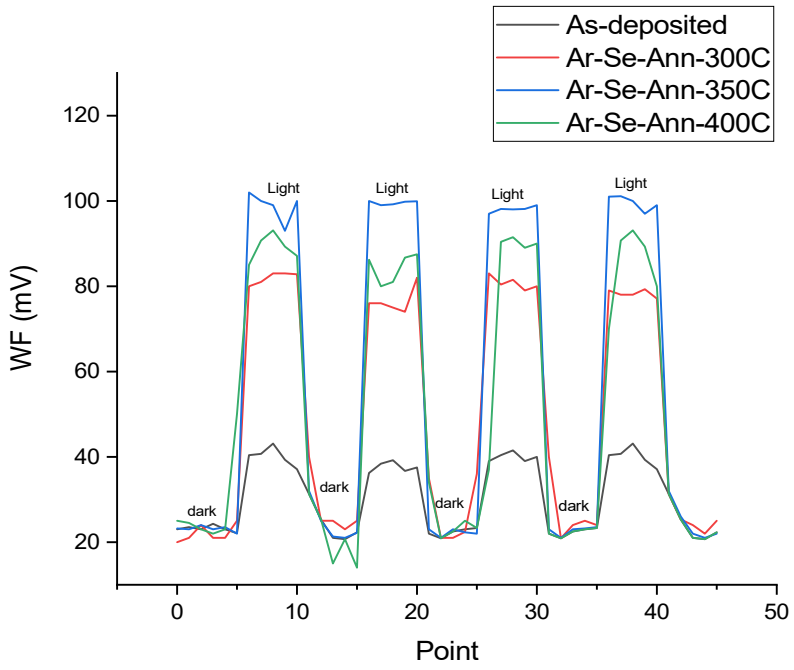

Figure 10 - Work function plot in light and dark for as-deposited films and films annealed in Ar-Se atmosphere.

3.2.5. Electrical properties.

The hot point probe method revealed that all annealed films have p-type conductivity. The resistivity of the annealed films is shown in fig. 15, there was a drop in resistivity from the film deposited at 300°C to that annealed in Ar-Se atmosphere at 300°C, a further decrease is notice as the annealing temperature increased, which could be linked to minor carrier concentration increasing. This result agrees with the XRD report, which shows an increase in grain sizes as the annealing temperature increases.

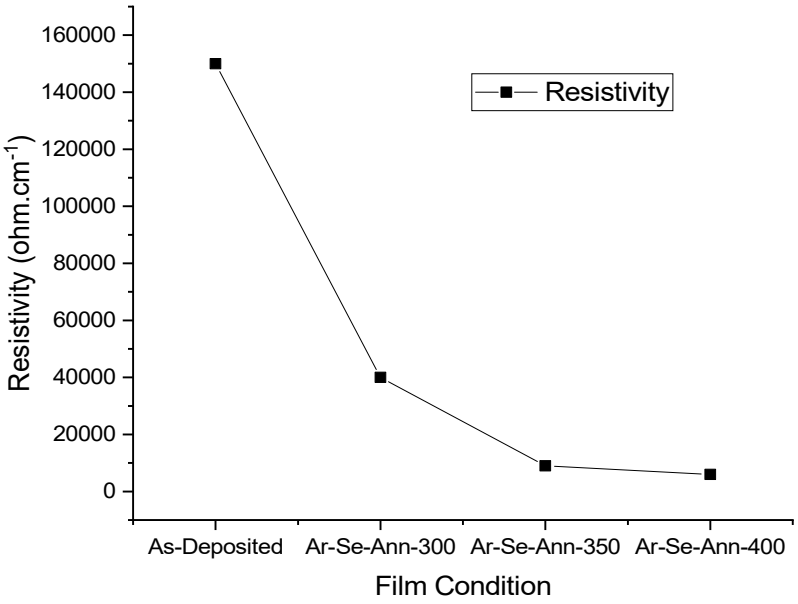

Figure 11 - Resistivity of films Annealed in Ar-Se atmosphere.

3.3. Solar cell properties.

Sb_2Se_3 thin films annealed in Ar-Se at 350°C was made into a complete solar cell (Fig. 12), all cell parameters were measured as described in section 2.5 of this work.

The I-V curve of this solar cell is shown in figure 13, the other cell parameters are as follows; short circuit current, I_{sc} of 11.6mA/cm^2 , open circuit voltage, V_{OC} of 233.85mV, Fill Factor, FF of 28.2% and Solar Cell Efficiency, η = 0.763%

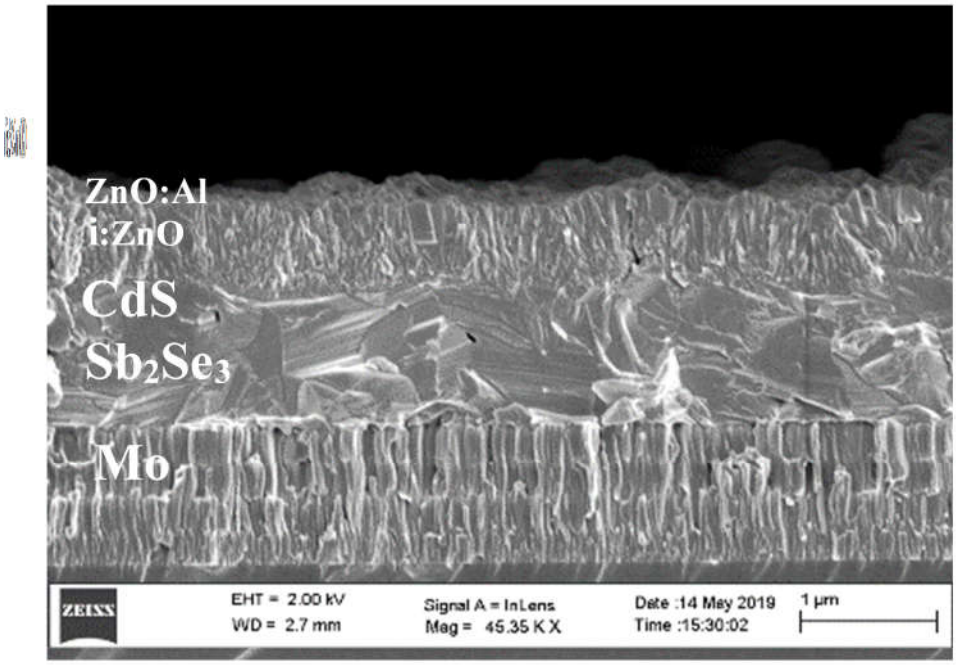

Figure 12 - SEM cross sectional image of the solar cell.

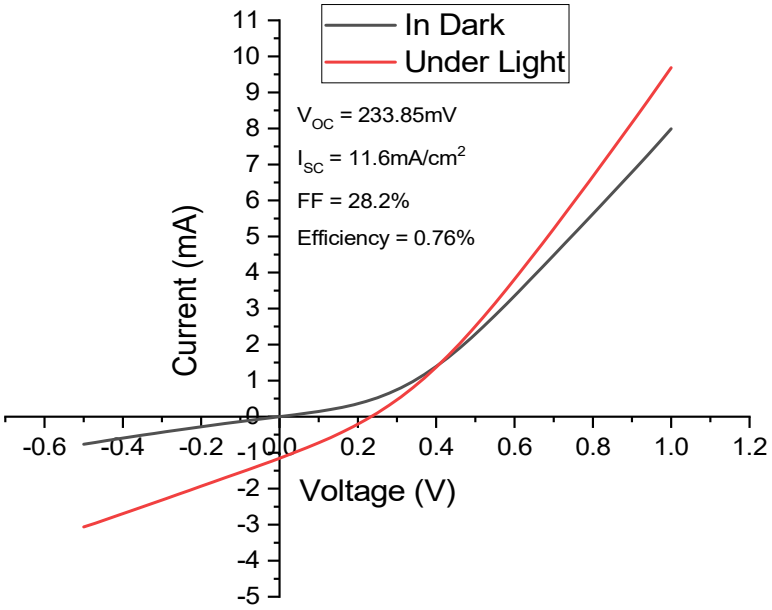

Figure 13 - I-V characteristics curve of the solar cell containing the Sb_2Se_3 film annealed in Ar-Se atmosphere at 350°C

CHAPTER FOUR: CONCLUSIONS AND RECOMMENDATION.

4.1. Conclusion.

This work has two main objectives, the first objective is to investigate the influence of substrate temperature on the properties of Sb_2Se_3 thin films produced by magnetron sputtering deposition technique. The second objective is to study the influence of post deposition annealing in Ar-Se atmosphere on the properties of the Sb_2Se_3 film. Sb_2Se_3 is a promising absorber material for photovoltaic cells. Only few investigations have been performed on Sb_2Se_3 films by magnetron sputtering which has a great potential to deposit uniform and well-adhered films. In the literature, there is still a lack of knowledge on suitable post-deposition treatment which could improve the film properties.

To summarize, the main findings from this work can be described as follows:

1. Magnetron sputtering can be employed for the deposition of uniform and well-adherent orthorhombic Sb_2Se_3 films in the temperature range of RT – 300^{o}C. As-deposited films were amorphous when grown at RT, and crystalline when grown at 200 and 300^{o}C.
2. All as-deposited Sb_2Se_3 films were selenium deficient compared to stoichiometric materials, exhibiting similar Sb/Se ratios of 1.0/1.4 and elemental compositions of ~42 at. % Sb to ~58 at. % Se regardless of substrate temperature applied.
3. Changing the substrate temperature from RT to 300^{o}C increased the crystallite size from amorphous material size to 56 nm, decreased the lattice parameters and optical bandgap values from 1.75 eV to 1.25 eV.
4. Post deposition thermal treatment in Ar-Se atmosphere at 300^{o}C for 30min improved slightly the crystallite size and the photosensitivity of Sb_2Se_3 films. Annealing performed at 300^{o}C yielded two-time higher photosensitivity than it was demonstrated by films as-deposited at 300^{o}C. Increasing the annealing temperature to 350^{o}C improved further the crystallite size and film photosensitivity. Annealing performed at 400^{o}C resulted in films with poor adhesion between Sb_2Se_3 and Mo substrates along with the formation of thick $MoSe_2$ layer.
5. This investigation revealed that Sb_2Se_3 films deposited at 300^{o}C and further annealed in Ar-Se atmosphere at 350^{o}C could be suitable for solar cell application. In order to demonstrate the film suitability to be used as an absorber material, a prototype solar cell with a configuration of

graphite/ZnO:AL/i-ZnO/CdS/Sb_2Se_3/Mo was prepared. This cell exhibited the solar parameters such as FF = 28.2%, I_{SC} = 1.157 mA, V_{OC} = 233.85 mV and the cell conversion efficiency of 0.76 %.

SUMMARY

Photovoltaic energy is one of the alternative sources of energy which will help the world in the transition process from fossils to other non-greenhouse emitting fuels, its availability, ease of use and maintenance are some of the reason for it being focused on. PV energy requires the use of solar cells for the conversion of the energy in the sun into electricity. Recent PV research has been focused on improving the efficiency of the solar cells and also replacing the toxic, expensive and limited available material with cheaper, more environmentally friendly and abundant materials. One of such material is Sb_2Se_3 which is the focus of this research.

Sb_2Se_3 is a very stable compound, with very suitable optical band gap for PV use, abundant with no toxicity and with very suitable electronic properties. It has been fabricated using different deposition techniques but very little has been done with magnetron sputtering deposition technique, which has the ability to produce uniform and well adhered films. It has also been reported that post deposition annealing is required to improve the overall film quality, several attempts has been made in different annealing atmosphere, however, there is still a lack of knowledge on suitable post-deposition treatment for this film. This is why this work is aimed at first investigating the influence of deposition temperatures on the properties of Sb_2Se_3 deposited by magnetron sputtering technique and secondly to study the influence of post deposition thermal treatment on the properties of the Sb_2Se_3 thin films.

In the first part of this work, thin films of Sb_2Se_3 about 1µm thick were deposited on soda lime glass and Mo coated soda lime glass substrates at substrate temperatures of RT, 200^{o}C and 300^{o}C. The properties of these films were then investigated using, XRD, Raman spectroscopy, SEM/EDS and UV-VIS spectroscopy. Result showed that film deposited at RT was amorphous, while there exist some crystallinity in the film deposited at 200^{o}C with small grain size, and the film deposited at 300^{o}C had big crystals and very compact and hole free, it is also worth noting that film deposited at temperatures higher than 300^{o}C did not deposit on the substrate. Bang gap of obtained films decreased from 1.75eV for the films deposited at RT to 1.25eV for the films deposited at 300^{o}C.

From the first part of this work, Sb_2Se_3 deposited at deposition temperature of 300^{o}C proved to be the best film. Hence, for the second part of this work, this film was annealed in Ar-Se atmosphere in isothermal sealed quartz ampoules at three different temperatures; 300^{o}C, 350^{o}C and 400^{o}C. all films were then characterized using XRD, Raman spectroscopy, SEM/EDS, UV-VIS spectroscopy, Kelvin probe technology

and Hot probe method. Result showed a further decrease in band gap value, improved photosensitivity, improvement in selenium deficiency and overall film quality as annealing temperatures increased. Film annealed in Ar-Se atmosphere at 350^{o}C had the best quality, this was then made into a solar cell with structure glass/Mo/Sb_2Se_3/CdS/ZnO/ZnO:Al/C and solar cell parameters; $I_{SC;}$ 11.6mA/cm^2, V_{OC}; 233.85mV, fill factor ; 28.2% and solar cell efficiency of 0.763%.

References

1. Ranabhat, K., Patrikeev, L., Antal'evna-Revina, A., Andrianov, K., Lapshinsky, V. and Sofronova, E., 2016. An introduction to solar cell technology. *Journal of Applied Engineering Science*, *14*(4), pp.481-491.

2. Sharma, S., Jain, K.K. and Sharma, A., 2015. Solar cells: in research and applications—a review. *Materials Sciences and Applications*, *6*(12), p.1145.

3. Kibria, M.T., Ahammed, A., Sony, S.M., Hossain, F. and Islam, S.U., 2014, September. A Review: Comparative studies on different generation solar cells technology. In *Proc. of 5th International Conference on Environmental Aspects of Bangladesh*.

4. Imamzai, M., Aghaei, M., Hanum Md Thayoob, Y. and Forouzanfar, M., 2012, November. A review on comparison between traditional silicon solar cells and thin-film CdTe solar cells. In *Proceedings of National Graduate Conference (Nat-Grad* (pp. 1-5).

5. Meindertsma, W. and Blok, K., 2014. Critical materials for the transition to a 100% sustainable energy future.

6. Haynes, W.M., 2014. CRC handbook of chemistry and physics. CRC press.

7. Norman, N.C. ed., 1997. Chemistry of arsenic, antimony and bismuth. Springer Science & Business Media.

8. Wang, C., 1909. Antimony: Its History, Chemistry, Mineralogy, Geology, Metallurgy, Uses Preparations, Analysis, Production, and Valuation; with Complete Biographies... JB Lippincott Company.

9. Ghosh, G., 1993. The Sb-Se (antimony-selenium) system. Journal of phase equilibria, 14(6), pp.753-763.

10. PDF, I., 2. Release 2008, Joint Committee on Powder Diffraction Standards (JCPDS)–International Centre for Diffraction Data (ICDD), Pennsylvania, 2008. *Powder Diffraction File (PDF) database*.

11. Madelung, O., 2012. *Semiconductors: data handbook*. Springer Science & Business Media.

12. Deringer, V.L., Stoffel, R.P., Wuttig, M. and Dronskowski, R., 2015. Vibrational properties and bonding nature of Sb 2 Se 3 and their implications for chalcogenide materials. Chemical science, 6(9), pp.5255-5262.

13. Jilani, A., Abdel-Wahab, M.S. and Hammad, A.H., 2017. Advance deposition techniques for thin film and coating. In *Modern Technologies for Creating the Thin-film Systems and Coating.* (pp. 137-149). InTech.

14. Liu, X., Chen, J., Luo, M., Leng, M., Xia, Z., Zhou, Y., Qin, S., Xue, D.J., Lv, L., Huang, H. and Niu, D., 2014. Thermal evaporation and characterization of Sb2Se3 thin film for substrate Sb2Se3/CdS solar cells. ACS applied materials & interfaces, 6(13), pp.10687-10695.

15. Kamruzzaman, M., Liu, C., Islam, A.F.U. and Zapien, J.A., 2017. A comparative study on the electronic and optical properties of Sb 2 Se 3 thin film. *Semiconductors*, *51*(12), pp.1615-1624.

16. Li, Z., Chen, X., Zhu, H., Chen, J., Guo, Y., Zhang, C., Zhang, W., Niu, X. and Mai, Y., 2017. Sb2Se3 thin film solar cells in substrate configuration and the back contact selenization. *Solar Energy Materials and Solar Cells*, *161*, pp.190-196.

17. Khrypunov, G., Romeo, A., Kurdesau, F., Bätzner, D.L., Zogg, H. and Tiwari, A.N., 2006. Recent developments in evaporated CdTe solar cells. Solar energy materials and solar cells, 90(6), pp.664-677.

18. Li, G., Li, Z., Chen, J., Chen, X., Qiao, S., Wang, S., Xu, Y. and Mai, Y., 2018. Self-powered, high-speed Sb2Se3/Si heterojunction photodetector with close spaced sublimation processed Sb2Se3 layer. Journal of Alloys and Compounds, 737, pp.67-73.

19. Hutter, O.S., Phillips, L.J., Durose, K. and Major, J.D., 2018. 6.6% efficient antimony selenide solar cells using grain structure control and an organic contact layer. Solar Energy Materials and Solar Cells, 188, pp.177-181.

20. Li, Z., Liang, X., Li, G., Liu, H., Zhang, H., Guo, J., Chen, J., Shen, K., San, X., Yu, W. and Schropp, R.E., 2019. 9.2%-efficient core-shell structured antimony selenide nanorod array solar cells. Nature communications, 10.

21. Swann, S., 1988. Magnetron sputtering. Physics in technology, 19(2), p.67.

22. Denton Vacuum, LLC. http://integral-storage.com/how-magnetron-sputtering-systems-enhance-deposition/ accessed on 08/04/2019.

23. Angstrom Engineering. https://angstromengineering.com/tech/magnetron-sputtering/ accessed on 08/04/2019.

24. Charpentier, C., 2012. Investigation of deposition conditions and annealing treatments on sputtered ZnO: Al thin films: Material properties and application to microcristalline silicon solar cells (Doctoral dissertation, Ecole Polytechnique X).

25. Liang, G.X., Zheng, Z.H., Fan, P., Luo, J.T., Hu, J.G., Zhang, X.H., Ma, H.L., Fan, B., Luo, Z.K. and Zhang, D.P., 2018. Thermally induced structural evolution and performance of Sb2Se3 films and nanorods prepared by an easy sputtering method. Solar Energy Materials and Solar Cells, 174, pp.263-270.

26. Chen, S., Hu, X., Tao, J., Xue, J., Weng, G., Jiang, J., Shen, X. and Chen, S., 2019. Effects of substrate temperature on material and photovoltaic properties of magnetron-sputtered Sb 2 Se 3 thin films. *Applied Optics*, *58*(11), pp.2823-2827.

27. Liang, X., Chen, X., Li, Z., Li, G., Chen, J., Yang, L., Shen, K., Xu, Y. and Mai, Y., 2019. Effect of deposition pressure on the properties of magnetron sputtering-deposited Sb 2 Se 3 thin-film solar cells. *Applied Physics A*, *125*(6), p.381.

28. Tang, R., Chen, X.Y., Liang, G.X., Su, Z.H., Luo, J.T. and Fan, P., 2019. Magnetron sputtering deposition and selenization of Sb2Se3 thin film for substrate Sb2Se3/CdS solar cells. Surface and Coatings Technology, 360, pp.68-72.

29. Yuan, C., Zhang, L., Liu, W. and Zhu, C., 2016. Rapid thermal process to fabricate Sb2Se3 thin film for solar cell application. *Solar Energy*, *137*, pp.256-260.

30. Razykov, T.M., Shukurov, A.X., Atabayev, O.K., Kuchkarov, K.M., Ergashev, B. and Mavlonov, A.A., 2018. Growth and characterization of Sb2Se3 thin films for solar cells. Solar Energy, 173, pp.225-228.

31. Martin, P.M., 2009. Handbook of deposition technologies for films and coatings: science, applications and technology. William Andrew.

32. Leng, M., Luo, M., Chen, C., Qin, S., Chen, J., Zhong, J. and Tang, J., 2014. Selenization of Sb2Se3 absorber layer: an efficient step to improve device performance of CdS/Sb2Se3 solar cells. *Applied Physics Letters*, *105*(8), p.083905.

33. Liu, X., Xiao, X., Yang, Y., Xue, D.J., Li, D.B., Chen, C., Lu, S., Gao, L., He, Y., Beard, M.C. and Wang, G., 2017. Enhanced Sb2Se3 solar cell performance through theory-guided

34. Shongalova, A., Correia, M.R., Teixeira, J.P., Leitão, J.P., González, J.C., Ranjbar, S., Garud, S., Vermang, B., Cunha, J.M.V., Salomé, P.M.P. and Fernandes, P.A., 2018. Growth of Sb2Se3 thin films by selenization of RF sputtered binary precursors. Solar Energy Materials and Solar Cells, 187, pp.219-226.

35. Rodríguez-Lazcano, Y., Peña, Y., Nair, M.T.S. and Nair, P.K., 2005. Polycrystalline thin films of antimony selenide via chemical bath deposition and post deposition treatments. *Thin Solid Films*, *493*(1-2), pp.77-82.

36. Maghraoui-Meherzi, H., Nasr, T.B. and Dachraoui, M., 2013. Synthesis, structure and optical properties of Sb2Se3. *Materials Science in Semiconductor Processing*, *16*(1), pp.179-184.

37. Vadapoo, R., Krishnan, S., Yilmaz, H. and Marin, C., 2011. Electronic structure of antimony selenide (Sb2Se3) from GW calculations. *physica status solidi (b)*, *248*(3), pp.700-705.

38. Kutasov, V.A., Lukyanova, L.N., Vedernikov, M.V. and Rowe, D.M., 2006. Shifting the maximum figure of merit of (Bi, Sb) 2 (Te, Se) 3 thermoelectrics to lower temperatures. Thermoelectrics Handbook: Macro to Nano, pp.37-1.

39. El-Sayad, E.A., 2008. Compositional dependence of the optical properties of amorphous Sb2Se3 xSx thin films. *Journal of Non-Crystalline Solids*, *354*(32), pp.3806-3811.

40. Xue, M.Z. and Fu, Z.W., 2008. Pulsed laser deposited Sb2Se3 anode for lithium-ion batteries. *Journal of Alloys and Compounds*, *458*(1-2), pp.351-356.

41. Kennison, R.E. and Stetson, W.J., International Business Machines Corp, 1975. Substrate cleaning process. U.S. Patent 3,898,351.

42. Martin, P.M., 2009. Handbook of deposition technologies for films and coatings: science, applications and technology. William Andrew.

43. Zhou, W. and Wang, Z.L. eds., 2007. *Scanning microscopy for nanotechnology: techniques and applications*. Springer science & business media.

44. Aharinejad, S.H. and Lametschwandtner, A., 1992. Fundamentals of Scanning Electron Microscopy. In Microvascular Corrosion Casting in Scanning Electron Microscopy (pp. 44-51). Springer, Vienna.

45. https://youtu.be/uQ1gCIkCbIQ. accessed 01/04/2019.

46. https://particle.dk/methods-analytical-laboratory/xrd-analysis/ accessed on 03/04/2019.

47. Speakman, S.A., 2014. Estimating crystallite size using XRD. MIT Center for Materials Science and Engineering.

48. Langford, J.I. and Wilson, A.J.C., 1978. Scherrer after sixty years: a survey and some new results in the determination of crystallite size. Journal of Applied Crystallography, 11(2), pp.102-113.

49. Patterson, A.L., 1939. The Scherrer formula for X-ray particle size determination. Physical review, 56(10), p.978.

50. Cullity, B.D. and Stock, S.R., 2001. Elements of X-ray diffraction third edition. Prenrice hall, New Jersey.

51. Chawla, K. (2013). Material Characterization Techniques.

52. Pujala, R.K., 2014. Materials and characterization techniques. In Dispersion Stability, Microstructure and Phase Transition of Anisotropic Nanodiscs (pp. 17-36). Springer, Cham.

53. Saini, V., Abdulrazzaq, O., Bourdo, S., Dervishi, E., Petre, A., Bairi, V.G., Mustafa, T., Schnackenberg, L., Viswanathan, T. and Biris, A.S., 2012. Structural and optoelectronic properties of P3HT-graphene composites prepared by in situ oxidative polymerization. Journal of Applied Physics, 112(5), p.054327.

54. El-Sayad, E.A., Moustafa, A.M. and Marzouk, S.Y., 2009. Effect of heat treatment on the structural and optical properties of amorphous Sb2Se3 and Sb2Se2S thin films. Physica B: Condensed Matter, 404(8-11), pp.1119-1127.

55. Chen, C., Li, W., Zhou, Y., Chen, C., Luo, M., Liu, X., Zeng, K., Yang, B., Zhang, C., Han, J. and Tang, J., 2015. Optical properties of amorphous and polycrystalline Sb2Se3 thin films prepared by thermal evaporation. Applied Physics Letters, 107(4), p.043905.

56. Hassanien, A.S. and Akl, A.A., 2015. Influence of composition on optical and dispersion parameters of thermally evaporated non-crystalline Cd50S50 xSex thin lms. Journal of Alloys and Compounds, 648, pp.280-290.

57. Revathi, N., Bereznev, S., Loorits, M., Raudoja, J., Lehner, J., Gurevits, J., Traksmaa, R., Mikli, V., Mellikov, E. and Volobujeva, O., 2014. Annealing effect for SnS thin films prepared by high-vacuum evaporation. *Journal of Vacuum Science & Technology A: Vacuum, Surfaces, and Films*, *32*(6), p.061506.

58. http://www.kelvinprobe.info/ (07/05/2019).

59. Wenham, S.R., Green, M.A., Watt, M.E., Corkish, R. and Sproul, A., 2013. *Applied photovoltaics*. Routledge.

60. Liu, C., Yuan, Y., Cheng, L., Su, J., Zhang, X., Li, X., Zhang, H., Xu, M. and Li, J., 2019. A study on optical properties of Sb2Se3 thin films and resistive switching behavior in Ag/Sb2Se3/W heterojunctions. *Results in Physics*, p.102228.

61. El Zawawi, I.K., Mahdy, M.A. and El-Sayad, E.A., 2017. Influence of Film Thickness and Heat Treatment on the Physical Properties of Mn Doped Sb2Se3 Nanocrystalline Thin Films. *Journal of Nanomaterials*, *2017*.

62. Ivanova, Z.G., Cernoskova, E., Vassilev, V.S. and Boycheva, S.V., 2003. Thermomechanical and structural characterization of GeSe2–Sb2Se3–ZnSe glasses. Materials Letters, 57(5-6), pp.1025-1028.

63. Shongalova, A., Correia, M.R., Vermang, B., Cunha, J.M.V., Salomé, P.M.P. and Fernandes, P.A., 2018. On the identification of Sb 2 Se 3 using Raman scattering. MRS Communications, 8(3), pp.865-870.

64. Tao, J., Hu, X., Xue, J., Wang, Y., Weng, G., Chen, S., Zhu, Z. and Chu, J., 2019. Investigation of electronic transport mechanisms in Sb2Se3 thin-film solar cells. Solar Energy Materials and Solar Cells, 197, pp.1-6.

65. Nagata, K., Ishibashi, K. and Miyamoto, Y., 1981. Raman and infrared spectra of rhombohedral selenium. Japanese Journal of Applied Physics, 20(3), p.463.